POAC'25
St. John's, Newfoundland and Labrador, Canada

Proceedings of the 28th International Conference on Port and Ocean Engineering under Arctic Conditions
Jul 13-17, 2025
St. John's, Newfoundland and Labrador
Canada

Traversability Analysis and Multivariate Optimal Path Planning in Dynamic Ice Fields

Md Ashiqul Alam Khan[1], Roger Skjetne[1], Ekaterina Kim[1]
[1]Norwegian University of Science and Technology, Trondheim, Norway

ABSTRACT

Arctic shipping routes are becoming increasingly viable due to climate change and the associated reduction of multi-year sea ice, creating both opportunities and challenges in global transportation. Effective path planning in ice-covered waters is essential to ensure navigational safety, minimize environmental risks, and optimize operational efficiency for vessels operating in these hazardous and dynamic environments. This proof-of-concept study aims to address the complexity of ice navigation by developing a unified multivariant path planning algorithm for areas with dynamic sea ice cover. We present a dynamic A* algorithm that integrates a custom cost function to account for ship-specific constraints and dynamic ice conditions in real-time. This custom cost function incorporates traversability of ice by evaluating ship resistance in open- and ice-covered water depending on the ship's characteristics, ice state, water salinity and temperature of ice, and ocean water. The algorithm integrates ship-specific constraints, such as ship's geometry, while also addressing simulated ice drift due to ocean currents and wind, ensuring that the path planning algorithm adapts to the dynamic environment. In this work, the position of sea ice cover is updated at each step using motion prediction from semi-realistic, simulated local observations and ice thickness profiles. We demonstrated the effectiveness of our algorithm in multiple scenarios that may arise in complex path planning situations. In addition, we have tested our method on a set of synthetic maps created from satellite imagery.

KEY WORDS: Dynamic A*; Ice Navigation; Ice Drift; Traversability Analysis

INTRODUCTION

The Arctic marine environment is undergoing significant changes due to the rapid loss of multi-year sea ice, leading to longer navigation seasons and access to previously unreachable areas. This has resulted in increased ship traffic in ice prone areas, raising concerns about maritime safety and management in the region (The Arctic Institute, 2023; Henke et al., 2024; WWF, 2024; Belfer Center, 2025). Given the dynamic and harsh nature of the Arctic environment, effective path planning is crucial for safe navigation. A robust path planning algorithm that can adapt to rapidly changing ice conditions, weather patterns, and other environmental factors can maximize the potential of Arctic shipping routes while minimizing operational risks.

The topics of traversability analysis and path planning have been extensively studied across multiple domains, with significant focus on ground-based systems as highlighted by Beycimen, Ignatyev, and Zolotas (2023). However, most conventional approaches often prioritize

obstacle-free navigation, neglecting critical traversability analyses, particularly in ice-covered waters (e.g., Bergman et al., 2020; Chiang et al., 2018; Shan et al., 2019; Choi et al., 2015; Aksakalli et al., 2017). While collision avoidance remains a core focus in these traditional maritime path planning, factors such as ice thickness and ship's interaction with rapidly changing ice cover are insufficiently addressed. While some works consider dynamic obstacles (e.g., Shah and Gupta, 2020; Stilman et al., 2008; Wu et al., 2010), they do not consider the physical interaction between the vehicle and moving ice fields.

Additionally, in the field of autonomous surface vehicle (ASV), path planning and collision avoidance have undergone extensive research, with many works focusing on static environments (Bergman et al., 2020; Shan et al., 2019) and some works that consider other floating objects as obstacles (Chiang et al., 2018; Zhuang et al., 2011; Kuwata et al. 2013). However, these approaches may not be directly applicable in areas with floating sea ice, where some collisions are inevitable. Choi et al. (2015) employed an uncertainty-based route planner for ship path planning, utilizing aggregated data on ice conditions obtained from satellite imagery. While their work encompasses planning pathways spanning several thousand kilometers, the absence of a dynamic map necessitates the incorporation of a local planner (10-20 Nm around the ship). This has been addressed by a proposed motion planner using data from marine radar imaging and bidirectional rapidly exploring random trees (RRT) (Hsieh et al., 2021). Gash et al. (2020) constructed a graph from a post-processed overhead image of an ice field, employing a morphological skeleton. Subsequently, the authors employed the A* algorithm to compute a path in the generated graph. Notably, the methodologies presented in Gash et al. (2020) and Hsieh et al. (2021) demonstrate good performance in simpler low concentration ice fields. However, challenges persist in addressing areas with high ice concertation and spatiotemporal ice drift. Schaetzen et al. (2023) in their paper have made significant strides in addressing ship interaction with smaller ice floes although without explicit consideration for traversing and breaking through the ice. Moreover, the smaller ice floes are treated as static entities within the local planning timeframe. This leaves a gap in the latter approach when confronted with the dynamic nature of larger ice floes and necessitates further exploration and refinement for a more realistic solution.

Segal et al. (2020) and Dammann et al. (2018) proposed methods to evaluate path traversability based on ice roughness in the Arctic; however, their research focuses solely on movement over ice rather than navigation through ice, such as by ships. Lu et al. (2024) introduced the high-traversability and efficient path optimization (HTEPO) strategy, leveraging an enhanced A* algorithm for efficient pathfinding in complex seabed environments for deep-sea mining vehicles. However, it lacks adaptability to dynamic maps and its traversability analysis is not directly applicable to ship navigation through ice-covered regions. Yaqing et al (2023) presented an algorithm where the ship is escorted by an icebreaker, although it is noteworthy that they did not delve into considerations of ice thickness or into calculating the traversability of ice cover. Tran et al. (2023) proposed a route optimization algorithm for vessels navigating ice-covered waters, incorporating carbon intensity based on ship resistance and ice thickness, while also factoring in ice type and associated risk levels for path planning. However, the model lacks a precise traversability index and does not account for the dynamic motion of ice. Zhang et al. (2019) developed a neural network-based model to predict energy efficiency and proposes an optimal route to minimize costs and environmental impact. While the model demonstrates strong alignment with real-world navigation, it does not account for dynamic map changes in Arctic conditions.

This paper tries to address these research gaps by incorporating ship-ice resistance (traversability) and ice motion (dynamicity) while focusing on independent navigation in ice.

Ship-specific constraints like turning rates have been omitted, the focus on dynamic environmental factors supports global-scale path optimization over distances exceeding 100 nautical miles.

METHODOLOGY

This section outlines the methodology used in the study. First, the path planning algorithm is introduced, and its functionality explained. Next, the custom cost function is detailed. Finally, the effectiveness of the algorithm is demonstrated using synthetic, dynamically changing traversable maps.

An A* algorithm (Hart et al., 1968) is implemented that searches the optimal path through a dynamic map (temporal sea ice positions) using a custom cost function. This cost function incorporates both open water resistance and the traversability resistance when the ship passes through traversable ice floes. The map is programmed to dynamically update the position of ice, adjusting at each time step based on the ship's current location during the search and the distance it has traveled over that duration. The proposed path planning algorithm can be systematically categorized into the following key components:

Dynamic A* Path Planning Algorithm:

The original A* search algorithm (for details refer to Hart et al., 1968) was implemented with some modifications, primarily incorporating additional cost function (traversability) and a set of time varying maps while searching for the optimal path. The algorithm aims to find a path (list of nodes) from the start position (*start_node*) to the goal position (*end_node*) with the smallest cost by searching among all possible paths within dynamic maps.

This modified A* search algorithm incorporates dynamic map updates and traversability costs for pathfinding in changing environments. This modification is particularly valuable when ice conditions change over time. The algorithm maintains two sets: an *open set* containing nodes to be evaluated and a *closed set* for already evaluated nodes. It uses a cost function $f(n) = g(n) + h(n)$, where $g(n)$ represents the actual cost from the start node to the current node, and $h(n)$ is a heuristic estimate of the cost from node n to the *end_node*. The algorithm periodically updates the grid *map* by utilizing a set of temporal datasets denoted by $\{M\}$, which includes predictive positions of ice floes across multiple time intervals. The map is updated based on the update frequency k.

In this traversability-aware path-finding algorithms, the equation $g_{\text{temp}} \leftarrow g(u) + d(u, v) \cdot \tau(v)$ calculates the temporary path cost to node v (neighbor node) through node u. This formulation integrates three critical components: $g(u)$, the accumulated cost from the start node to the current node u; $d(u, v)$, the base distance between adjacent nodes; and $\tau(v)$, a traversability cost multiplier that accounts for ship resistance in ice.

Pseudocode for dynamic A* path planning algorithm:

Input: *start_node*, *end_node*, set of maps$\{M\}$

Output: path P

A* $(start\_node, end\_node, \{M\})$:

Initialize:

open set $\leftarrow \{start\_node\}$

closed set $\leftarrow \emptyset$

$\partial t \leftarrow 0$ map-update time

$g(start\_node) \leftarrow 0$
$h(start\_node) \leftarrow H(start\_node, end\_node)$
$f(start\_node) \leftarrow g(start\_node) + h(start\_node)$
$map \leftarrow \{M(\partial t)\}$
$\forall n \in$ Map: $\tau(n) \leftarrow map\ (n)$
while open set $\neq \emptyset$ **do**
  $u \leftarrow \arg\min_{n \in \text{open}} f(n)$
  if $u = end\_node$ then
    return ReconstructPath(u)
  end if
  open set $\leftarrow$ open set $\setminus \{u\}$
  closed set $\leftarrow$ closed set $\cup \{u\}$
  if |ReconstructPath(u)|mod$k = 0$ **then**
    UpdateMap$(u,\ \{M\})$
  end if
  $\forall v \in$ Adj(u):
    if $v \in$ closed set **then continue**
    end if
    $g_{\text{temp}} \leftarrow g(u) + d(u, v) \cdot \tau(v)$
    if $v \notin$ open set **then**
    open set $\leftarrow$ open set $\cup \{v\}$
    end if
    else if $g_{\text{temp}} \geq g(v)$ **then continue**
    parent$(v) \leftarrow u$
    $g(v) \leftarrow g_{\text{temp}}$
    $h(v) \leftarrow h(v, end\_node)$
    $f(v) \leftarrow g(v) + h(v)$
return $\emptyset$

ReconstructPath(u):
  $P \leftarrow \langle u \rangle$
  while $\exists$ parent(u) **do**
    $u \leftarrow$ parent(u)
    $P \leftarrow \langle u \rangle.append(P)$
return P

UpdateMap($u, \{M\}$):
  $\partial t = |\text{ReconstructPath}(u)|//k$
return $\{M(\partial t)\}$

$g(n)$ cost of the node *n*
$h(n)$ heuristic cost of the node *n*
$f(n)$ total cost of the node *n*
$\tau(n)$ traversability cost for node *n*
u – current node
k – map update frequency
v – current node neighborhood
d is a travel distance cost between neighboring nodes *u* and *v*

Cost Function:

The methodology detailed assumed a uniform ice floe thickness for simplified simulation process. Different ice floes can have different thickness. The traversal cost integrates both the ice-to-open-water resistance ratio and path distance, quantified through a comprehensive

traversability metric. To ensure goal-oriented navigation, distance heuristic was incorporated to prioritize paths advancing toward the target destination. This approach balances efficiency and safety by leveraging adaptive path planning informed by ice resistance dynamics and spatial constraints.

Heuristics Cost

Distance heuristics were used in the A* algorithm to lead the path towards the goal. A straightforward form of Euclidean distance heuristics was implemented according to:

$$H(x, y) = W \cdot \sqrt{(x_{goal} - x)^2 + (y_{goal} - y)^2} \quad (1)$$

where, (x, y) is the current node coordinate and (x_{goal}, y_{goal}) is the goal node coordinate. Thus, the calculated heuristics cost of the current node $H(x, y)$ is represented in pixel distance from the goal node. We set the weight value W assigned to the $H(x, y)$ heuristics cost to one as default.

Traversability Cost:

One of the main contributions of this paper is to enhance the traditional A* algorithm with traversability cost. This cost was computed by evaluating the ratio between the resistance of a ship on a traversable path and their resistance in open water, considering a constant ship speed. The ship resistance was determined using the methodology outlined in the papers from Keinonen et al. (1991) and Frederking et al. (2003). In this paper, the same notations as in Frederking et al. (2003) were used. Based on that, the total resistance of a ship in level ice was calculated by

$$R_{ice} = R_{ice}(V_{ms} = 1) + R_{ice}(V_{ms}>1) + R_{water} \quad (2)$$

where, R_{ice} is the total resistance of the ship in the level ice.

The ice resistance for ship velocity normalized to 1 m/s $R_{ice}(V_{ms}=1)$ is calculated based on Eq. (3) that is,

$$R_{ice}(V_{ms} = 1) = 0.015\, HC \cdot S \quad (3)$$

$$\times B^{0.7} L^{0.2} D^{0.1} h_{eq}{}^{1.5} \qquad \text{ship size term}$$

$$\times\left(1 - 0.0083(T + 30)\right) \qquad \text{friction term}$$

$$\times(0.63 + 0.00074\sigma_f) \qquad \text{ice strength term}$$

$$\times(1 + 0.0018(90 - \gamma)^{1.6})(1 + 0.003(\beta - 5)^{1.5}) \qquad \text{bow term}$$

Here, the hull condition factor is represented by HC with value of 1, the factor for water salinity is denoted by S with a value of 0.85, the ship beam is given by B with a measurement of 22 meters, the waterline length of the ship is denoted by L which is equal to 147 meters, the draft is represented by D with a value of 6.9 meters, the equivalent ice thickness is expressed as h_{eq} in meters and was defined as in Frederking et al. (2003) which takes into account a constant snow thickness of 0.1 meter, the ice surface temperature is represented by T and was assumed -10 degree Celsius, the flexural strength of ice is denoted by σ_f (350 kPa), the average bow flare angle at the waterline is expressed as γ (21 degrees), and the average buttock angle at the waterline is represented by β (32 degrees). It is important to note that all the terms are multiplied together.

Ice resistance for ship velocity greater than 1 m/s $R_{ice}(V_{ms}>1)$ is calculated by

$$R_{ice}(V_{ms}>1) = 0.009HC(\Delta V/(gL)^{0.5}) \quad (4)$$

$\times B^{1.5}D^{0.5}H_i$ ship size term

$\times\left(1 - 0.0083(T+30)\right)$ friction term

$\times(1+0.0018(90 - \gamma)^{1.6})(1 + 0.003(\beta - 5)^{1.5})$ bow term

where, $\Delta V = V - 1 (\text{m/s})$ and $g = 9.81 \text{m/s}^2$

Open water ship resistance was calculated using Eq. (5).

$$R_{water} = \delta^{1.1}\left(0.025F_n + 8.8F_n^5\right)/1000 \quad (5)$$

where,

$\delta = \rho_w LBDC_b (\text{tonnes})$

$\rho_w = 1.03$ tonnes/m^3 weight density of sea water

C_b block coefficient

$F_n = V/(gL)^{0.5}$ Froude number

The final cost for each ice floe node can be expressed as:

$$\tau(n) = R_{ice}/R_{water} \quad (6)$$

where, $\tau(n)$ is the ice floe traversability cost with $\tau(n) = 1$ when the ship is in open water.

Map Creation:

To create a semi-realistic input map, real-world satellite images are used, converting them into a 2D ice-water binary maps. To enhance the complexity of the ice field, instead of stitching several satellite tiles together, a rectangular area of around 10×6 Nm was selected from the satellite image, and it was upscaled to a larger area (100×60 Nm). The selection of this area was based on a qualitative assessment, considering increased complexity and the availability of multiple traversable paths as perceived by human observation inspective of land ice-, sea ice-, and cloud coverage. Three Sentinel-2 images (RGB - channels) of shape 1600×900pixels were acquired from Copernicus (Copernicus Sentinel data, 2024), focusing on the coast of Greenland. Thus, after upscaling, each pixel corresponded to a single cell with an area of 0.4166 Nm² in the grid map which was then utilized by our path planning algorithm. The resulting RGB image was initially converted into a grayscale representation for further processing. All areas near black were assigned a value of zero, representing open water, while brighter surfaces were set to 255, indicating level ice and ice floes. In addition, to eliminate any thin connecting joints between ice floes while preserving the shape of larger ice floes, we applied erosion followed by dilation morphological operations on the image (for details refer to Serra, 1982).

The resulting binary image is shown in Fig. 1, where different ice floes were assigned to different thickness as explained below.

Thickness Map:

Ideally, a thickness map should be derived using sensor fusion, combining e.g., high-resolution lidar measurements from ships for local characterization, with marine/coastal radar(s) and satellite data providing broader spatial coverage. In the absence of actual thickness data, for simplicity, a synthetic thickness map was created by randomly assigning ice thickness values ranging from 0.1 meters (new ice) to 3 meters (multiyear ice) across various ice floes based on data from Polar Portal (2025). The broader range was chosen to enhance variability in the available traversable paths, allowing for a more comprehensive evaluation of potential routes. This approach created a spatially uniform yet random distribution of ice thickness across the map (see Fig. 1).

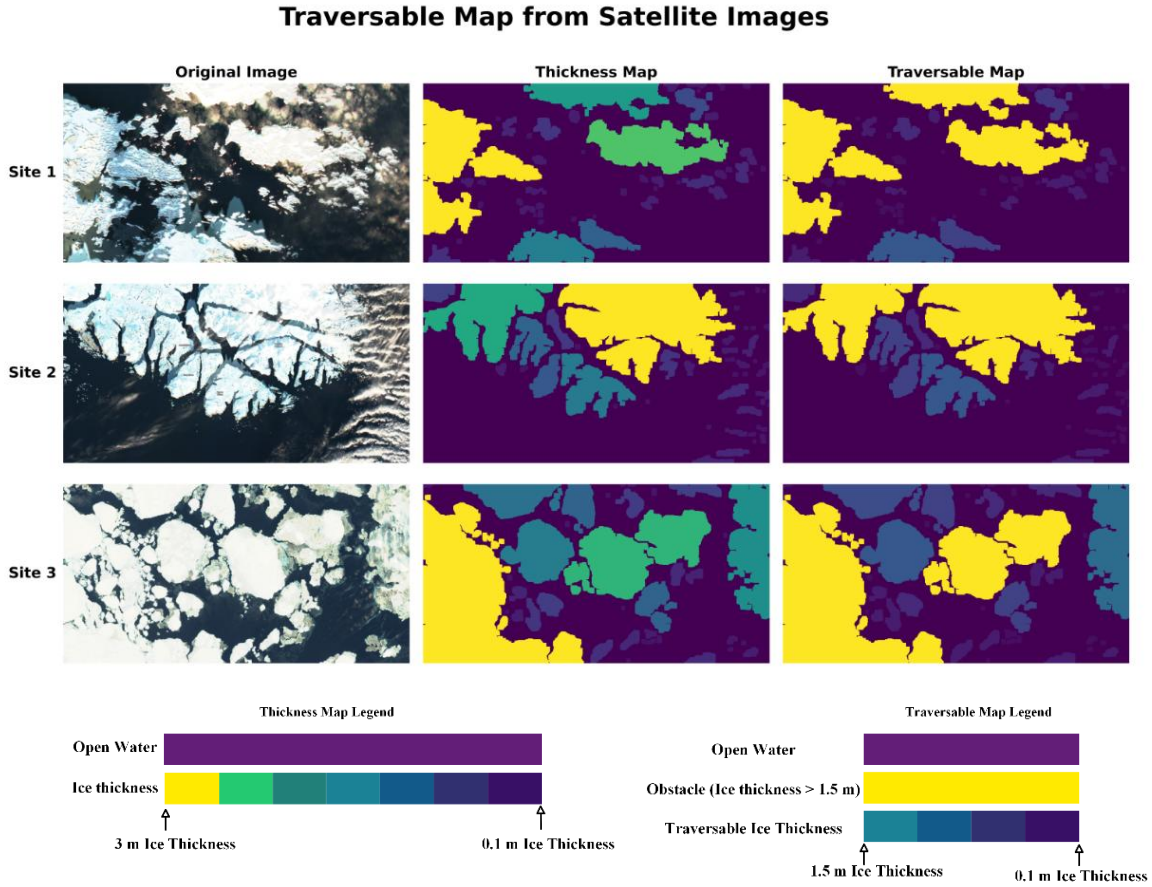

Figure 1. Synthetic map creation from satellite data, showcasing the transformation from the original RGB image to the thickness map and traversability map across various sites.

Traversable and Obstacle Map:

Following the generation of the thickness map, ice floes were categorized as traversable or non-traversable based on their resistance to ship movement relative to open water resistance based on Eq. 6. This classification integrates both ice thickness and ship-specific characteristics. Under the assumption of constant ice material properties (only for the algorithm demonstration purposes), thickness becomes the critical variable governing traversability.

A traversability threshold was established by comparing ice resistance to open water resistance. Ice floes with resistance values greater than ten times the values compared to open water resistance were assumed non-traversable. These resistance values formed the basis of our traversability cost function, which quantifies navigation challenges across varying ice conditions. Figure 1 provides a representative visualization of this classification process

applied to generate the synthetic ice map.

Dynamic Map:

Ideally, the information about ice drift should be utilized in field applications. In this study, to account for the dynamic nature of the ice cover, a function was introduced that adjusts the map based on the time the ship has traveled from its initial position. This function takes into consideration the ice velocity of individual floes, which was assumed to be uniform. To ensure a more accurate representation of directional changes, a two-pixel shift was implemented for each iteration of movement (see Fig. 2).

Given the uncertainty beyond the boundary of the initial image (areas not known to us when the algorithm will run), any shift of values outside this boundary was considered an obstacle and was accordingly adjusted (visible as a yellow straight line around the respective boundary based on the directional movement). After a predefined iteration of the A* search, updated the map and continued the A* search on the modified map.

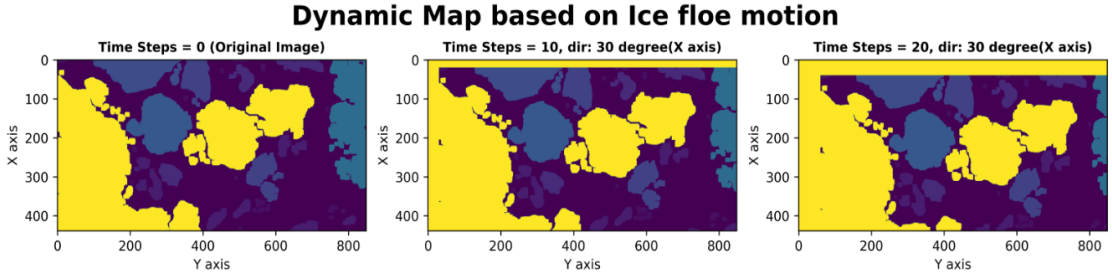

Figure 2. Illustration of the map evolution for three time periods. It shows the predicted positions of ice floes as time progresses.

RESULTS

The effectiveness of the algorithm depends on both the type of map used and the positions of the start and goal nodes. Due to the variability in map diversity and start-goal configuration, the algorithm's effectiveness is theoretically grounded rather than reliant on specific input data. The input map serves to demonstrate the algorithm's performance in various scenarios and should be viewed as a proof-of-concept.

Figure 3 compares the optimal paths generated by three approaches: the original A* search, A* with traversability cost, and A* with traversability cost plus a dynamic map. At Site 1, A* with traversability cost produced a shorter path (69.10 Nm) than the original A* (82.99 Nm), with a length ratio of 0.832. The dynamic map further reduced the path to 68.48 Nm (ratio 0.825).

At Site 2, A* with traversability cost reduced the path from 53.43 Nm to 45.76 Nm (ratio 0.856), and the dynamic map further optimized it to 44.98 Nm (ratio 0.842).

At Site 3, the original A* path was 229.08 Nm; A* with traversability cost reduced it to 94.30 Nm (a 58.8% reduction), and the dynamic map further shortened it to 81.12 Nm, representing a 64.6% reduction compared to the original A* and a 13.97% reduction compared to A* with traversability cost.

Table 1. Comparison of Path Planning Algorithms: Path Length and Efficiency Across Three Test Sites (Path length is expressed as $l = d(n) \cdot \tau(n),\ n \in P$)

Site No (i)	Output Path Length in Nm		
	A*	A* + Traversability	A* + Traversability + Dynamic Map

	Length $l(i)$ Nm	Length $l_t(i)$ Nm	Ratio $l_t(i)/l(i)$	Length $l_{td}(i)$ Nm	Ratio $l_{td}(i)/l(i)$
Site 1	82.99	69.10	0.832	68.48	0.825
Site 2	53.43	45.76	0.856	44.98	0.842
Site 3	229.08	94.30	0.412	81.12	0.354

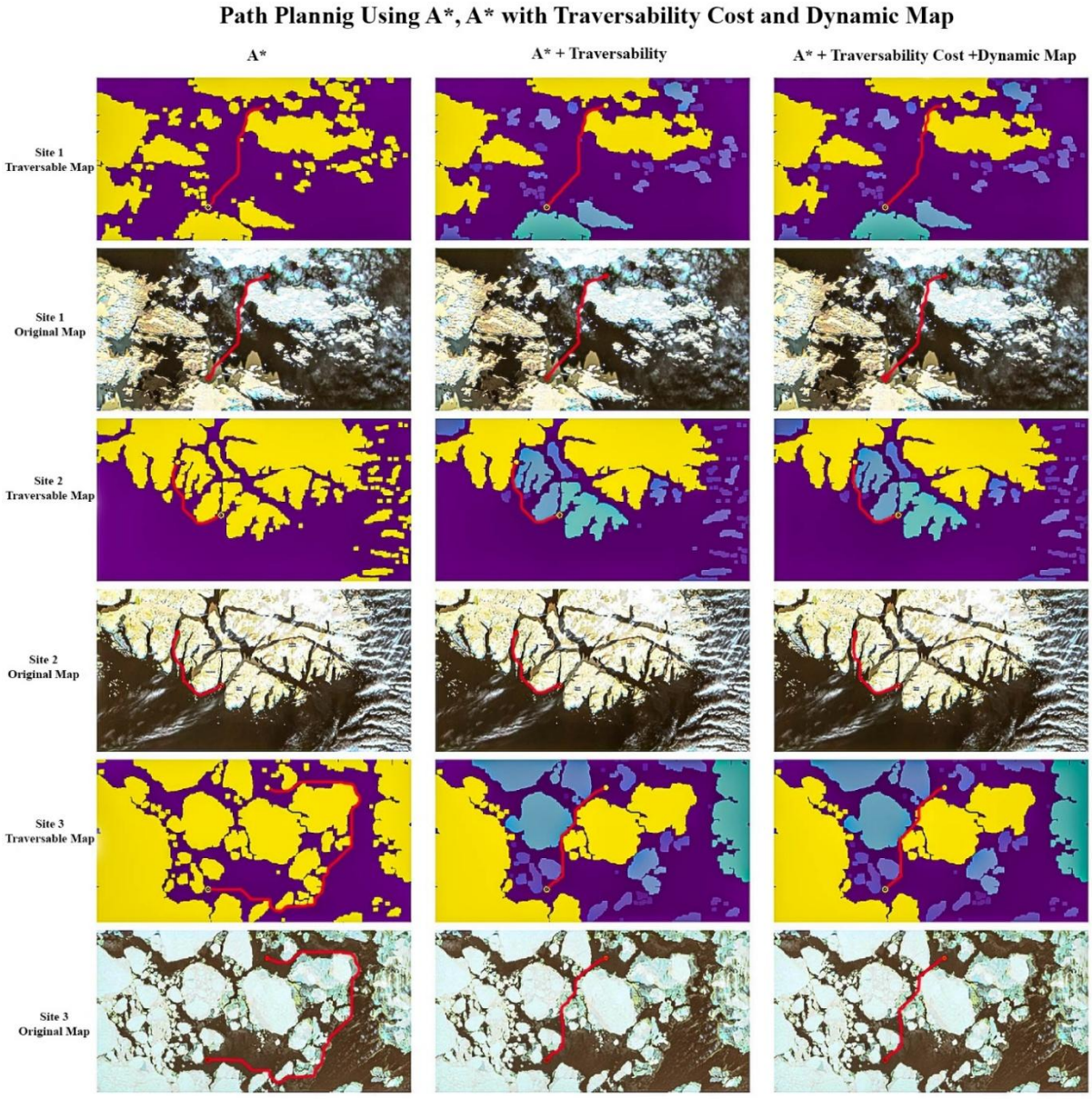

Figure 3. Comparison of A* path planning algorithms with and without traversability and dynamic mapping. The empty circle represents the start position, while the filled circle denotes the goal position.

Our algorithm possesses the following key characteristics:

1. Optimality: The algorithm ensures path optimality within the modeled constraints by

employing admissible heuristics and evaluating all traversable paths on the map. This optimality is contingent on the defined cost function and environmental assumptions (e.g., ice dynamics, ship resistance parameters) used in the study.

2. Traversability: A key quality of our algorithm is the incorporation of traversability, which allows for the identification of additional paths through the ice rather than treating ice as non-traversable obstacles. This makes our algorithm more versatile compared to traditional path planning methods that rely solely on a non-traversable obstacle map.
3. Adaptability to dynamic environments: The dynamic nature of our map plays a crucial role in reducing the risk of collision with non-traversable objects compared to static maps. The dynamic map not only enhances safety but also provides a shorter path, demonstrating that a dynamic map significantly improves both path efficiency and safety (ref. Fig. 3 Site 3)

These results consistently show that incorporating traversability cost and dynamic mapping leads to shorter and more efficient paths across all three sites, with Site 3 exhibiting the most dramatic improvement. Incorporating traversability cost always provides shorter paths but may not be always collision free due to the absence of dynamic maps, and traversability cost with dynamic map always leads to much more safer paths and reduces any occurrence of collision. Thus, it is the only algorithm that provides shortest collision free path among the 3 algorithms tested. Based on prioritizing safety first and then path length, A* with traversability and dynamic map consistently produces the most optimal path, balancing both critical navigation requirements.

CONCLUSIVE REMARKS

In this proof-of-concept work, we have developed a model that successfully identifies optimal paths by integrating critical information on ice size, thickness and flexural strength, enabling a comprehensive traversability analysis. The incorporation of a traversability cost function has proven to be highly effective, resulting in the generation of shorter and more efficient paths compared to the original A* algorithm, which only considered heuristics and motion costs.

Moreover, the introduction of a dynamic map significantly improves the situational awareness in terms of future path predictions while adapting to changes in the ice cover. This dynamic model predictive mapping approach not only improves the traditional A* search algorithm but also offers enhanced flexibility in response to evolving conditions. Despite these advancements, there remain potential avenues for further refinement. One promising direction involves the implementation of a Hybrid A* algorithm, which will improve path planning to adhere with ship maneuverability and more effectively address dynamic constraints associated with ship motion during pathfinding.

Additionally, the domain of traversability analysis, particularly in relation to in-situ ice thickness prediction through sensor data, and ice floe tracking through radar and satellite data present substantial opportunities for further research. Continued exploration of this research domain will help to refine and enhance the model, making it more robust and accurate in generating optimal paths under varying Arctic conditions.

The implemented ice resistance formulations are semi-empirical and may not be suited for high fidelity modelling (e.g. in ice ridge fields). Added resistance due to wind and waves was not considered. Following the advancements made in ship performance evaluation in open water conditions, there is potential to refine current ice resistance formulations (e.g., a data-driven approaches provided a rich history of operating in ice on a well instrumented vessel for ice conditions monitoring).

ACKNOWLEDGEMENT

This research was supported by the DigitalSeaIce project (Project No. 328960), funded by the Research Council of Norway.

REFERENCES

Aksakalli, V., Oz, D., Alkaya, A.F. and Aydogdu, V., 2017. Optimal naval path planning in ice-covered waters. *International Journal of Maritime Engineering*, 159(A1).

Belfer Center, 2025. *Arctic Shipping: Trends, Challenges and Ways Forward*. [Online] Available at: https://www.belfercenter.org/publication/arctic-shipping-trends-challenges-and-ways-forward [Accessed: 5 Jan 2025].

Bergman, K., Ljungqvist, O., Linder, J. and Axehill, D., 2020. An optimization-based motion planner for autonomous maneuvering of marine vessels in complex environments. *IEEE Conference on Decision and Control*, Jeju, Korea (South), 2020, pp.5283–5290.

Beycimen, S., Ignatyev, D. and Zolotas, A., 2023. A comprehensive survey of unmanned ground vehicle terrain traversability for unstructured environments and sensor technology insights. *Engineering Science and Technology, an International Journal*, 47, p.101457.

Chiang, H.-T.L. and Tapia, L., 2018. COLREG-RRT: An RRT-based COLREGS-compliant motion planner for surface vehicle navigation. *IEEE Robotics & Automation Letters*, 3(3), pp.2024–2031.

Choi, M., Chung, H., Yamaguchi, H. and Nagakawa, K., 2015. Arctic sea route path planning based on an uncertain ice prediction model. *Cold Regions Science and Technology*, 109, pp.61–69.

Copernicus Sentinel data, 2024. *Greenland, Copernicus Data Space Ecosystem*. [Online] Available at: https://dataspace.copernicus.eu/ [Accessed: 15 December 2024]

Dammann, D.O., Eicken, H., Mahoney, A.R., Saiet, E., Meyer, F.J. and George, J.C., 2018. Traversing sea ice-Linking surface roughness and ice trafficability through SAR polarimetry and interferometry. *IEEE Journal of Selected Topics in Applied Earth Observations and Remote Sensing*, 11(2), pp.416–433.

De Schaetzen, R., Botros, A., Gash, R., Murrant, K. and Smith, S.L., 2023. Real-time navigation for autonomous surface vehicles in ice-covered waters. *IEEE International Conference on Robotics and Automation (ICRA)*, London, United Kingdom, 2023, pp.1069–1075.

Frederking, R., 2003. A model for ship routing in ice. In: Proceedings of the International *Conference on Port and Ocean Engineering Under Arctic Conditions (POAC'03)*, Trondheim, Norway, 2003, vol. 2, pp.467–476.

Gash, R.M., Murrant, K.A., Mills, J.W. and Millan, D.E., 2020. Machine vision techniques for situational awareness and path planning in model test basin ice-covered waters. *Global Oceans 2020: Singapore – U.S. Gulf Coast*. pp.1–8.

Hart, P.E., Nilsson, N.J. and Raphael, B., 1968. A formal basis for the heuristic determination of minimum cost paths. *IEEE Transactions on Systems Science and Cybernetics*, 4(2), pp.100–107.

Henke MT, Miesse T, de Souza de Lima A, Ferreira C, Ravens T, Pundt R., 2024. Evolving Arctic maritime hazards: Declining sea ice and rising waves in the Northwest Passage. *Proceedings of the National Academy of Sciences of the United States of America*, 121(29), p. e2400355121.

Hsieh, T.-H., Wang, S., Gong, H., Liu, W. and Xu, N., 2021. Sea ice warning visualization and path planning for ice navigation based on radar image recognition. *Journal of Marine Science and Technology*, 29(3), pp.280–290.

Keinonen, A., Browne, R.P. and Revill, C.R., 1991. Icebreaker design synthesis: Phase 2: Analysis of contemporary icebreaker performance. *Arno Keinonen Arctic Consulting Incorporated*.

Kuwata, Y., Wolf, M.T., Zarzhitsky, D. and Huntsberger, T.L., 2013. Safe maritime autonomous navigation with COLREGS, using velocity obstacles. *IEEE Journal of Oceanic Engineering*, 39(1), pp.110–119.

Lu, C., Yang, J., Leira, B.J., Skjetne, R., Mao, J., Chen, Q. and Xu, W., 2024. High-traversability and efficient path optimization for deep-sea mining vehicles considering complex seabed environmental factors. *Ocean Engineering*, 313(Part 2), p.119500.

Polar Portal, 2025. *Sea ice thickness and volume*. Danish Meteorological Institute. [Online] Available at: https://polarportal.dk/en/sea-ice-and-icebergs/sea-ice-thickness-and-volume/ [Accessed: 22 January 2025].

Segal, R.A., Scharien, R.K., Duerden, F. and Tam, C., 2020. Connecting remote sensing and Arctic communities for safe sea ice travel. *Arctic*, 73(4), pp.461–484.

Serra, J., 1982. *Image analysis and mathematical morphology*. London: Academic Press.

Shah, B.C. and Gupta, S.K., 2020. Long-distance path planning for unmanned surface vehicles in complex marine environments. *IEEE Journal of Oceanic Engineering*, 45(3), pp.813–830.

Shan, T., Wang, W., Englot, B., Ratti, C. and Rus, D., 2020. A receding horizon multi-objective planner for autonomous surface vehicles in urban waterways. *IEEE Conference on Decision and Control*, Jeju, Korea (South), 2020, pp.4085–4092.

Shu, Y., Zhu, Y., Xu, F., Gan, L., Lee, P., Yin, J. and Chen, J., 2023. Path planning for ships assisted by the icebreaker in ice-covered waters in the Northern Sea Route based on optimal control. *Ocean Engineering*, 267, p.113182.

Stilman, M. and Kuffner, J., 2008. Planning among movable obstacles with artificial constraints. *The International Journal of Robotics Research*, 27(11–12), pp.1295–1307.

The Arctic Institute, 2023. *The Future of the Northern Sea Route – A "Golden Waterway" or a Niche?* [Online] Available at: https://www.thearcticinstitute.org/future-northern-sea-route-golden-waterway-niche/ [Accessed 5 Jan 2025].

Tran, T.T., Browne, T., Veitch, B., Musharraf, M. and Peters, D., 2023. Route optimization for vessels in ice: Investigating operational implications of the carbon intensity indicator regulation. *Marine Policy*, 158, p.105858.

Wu, H.-N., Levihn, M. and Stilman, M., 2010. Navigation among movable obstacles in unknown environments. *IEEE/RSJ International Conference on Intelligent Robots and Systems*, Taipei, Taiwan, 2010, pp.1433–1438.

WWF, 2024. *Shipping*. [Online] Available at: https://www.arcticwwf.org/threats/shipping/ [Accessed: 5 Jan 2025].

Zhang, C., Zhang, D., Zhang, M. and Mao, W., 2019. Data-driven ship energy efficiency analysis and optimization model for route planning in ice-covered Arctic waters. *Ocean Engineering*, 186, p.106071.

Zhuang, J.-Y., Su, Y.-M., Liao, Y.-L. and Sun, H.-B., 2011. Motion planning of USV based on marine rules. *Procedia Engineering*, 15, pp.269–276.